

- (19) R. G. Snyder and G. Zerbi, *Spectrochim. Acta, Part A*, **23**, 391 (1967).
- (20) G. N. Ramachandran and C. M. Venkatachalam, *Biopolymers*, **6**, 1255 (1968).
- (21) M. Bixon and S. Lifson, *Tetrahedron*, **23**, 769 (1967).
- (22) M. H. Liberman, L. C. DeBolt, and P. J. Flory, *J. Polym. Sci., Polym. Phys. Ed.*, **12**, 187 (1974).
- (23) C. W. Bunn and D. R. Holmes, *Discuss. Faraday Soc.*, **25**, 95 (1958).
- (24) P. Corradini, "Stereochemistry of Macromolecules", Vol. 3, A. D. Ketley, Ed., Marcel Dekker, New York, N.Y., 1968, p 1.
- (25) T. Miyazawa, ref 24, p 147.
- (26) D. R. Lide, Jr., *J. Chem. Phys.*, **33**, 1519 (1960).
- (27) D. W. Marquardt, *J. Soc. Ind. Appl. Math.*, **11**, 431 (1963).
- (28) R. A. Scott and H. A. Scheraga, *J. Chem. Phys.*, **44**, 3054 (1966).
- (29) U. Biskup and H.-J. Cantow, *Makromol. Chem.*, **168**, 315 (1973).
- (30) Y. Fujiwara and P. J. Flory, *Macromolecules*, **3**, 280 (1970).
- (31) A. Abe, *Polym. J.*, **1**, 232 (1970).
- (32) A. E. Tonelli, unpublished results.
- (33) A. Zambelli, A. Segre, M. Farina, and G. Natta, *Makromol. Chem.*, **110**, 1 (1967).
- (34) F. Heatley, R. Salovey, and F. A. Bovey, *Macromolecules*, **2**, 619 (1969).
- (35) P. J. Flory, *Macromolecules*, **3**, 613 (1970).
- (36) J. B. Kinsinger and R. E. Hughes, *J. Phys. Chem.*, **67**, 1922 (1963).
- (37) J. C. Randall, *J. Polym. Sci., Polym. Phys. Ed.*, **12**, 703 (1974).
- (38) H. Inagaki, T. Miyamoto, and S. Ohta, *J. Phys. Chem.*, **70**, 3420 (1966).
- (39) G. Natta, I. Pasquon, and A. Zambelli, *J. Am. Chem. Soc.*, **84**, 1488 (1962).
- (40) K. Mitani, T. Suzuki, A. Matsuo, and Y. Takegami, *J. Polym. Sci., Polym. Chem. Ed.*, **12**, 771 (1974).
- (41) F. Hamada, unpublished.
- (42) T. Asakura, I. Ando, and A. Nishioka, *Makromol. Chem.*, **176**, 1151 (1975).

## Conformational Characteristics of Polystyrene

D. Y. Yoon, P. R. Sundararajan, and P. J. Flory\*

Department of Chemistry, Stanford University, Stanford, California 94305.

Received June 16, 1975

**ABSTRACT:** Conformational energies of meso and racemic dyads of polystyrene have been computed as functions of skeletal bond rotations. Confinement of rotations of the phenyl groups to a small range within which they are nearly perpendicular to the plane defined by the two adjoining skeletal bonds is confirmed. Steric interactions involving the relatively large planar phenyl group virtually preclude  $\bar{g}$  conformations. Four prominent minima, denoted tt, gg, tg, and gt, are indicated for both meso and racemic dyads. The energy of the meso;tt state, in which the phenyl groups are apposed and in close proximity, is much reduced by shifts in the torsion angles from 0,0° (for perfect staggering) to 20,20°, the latter being the location of the meso;tt minimum according to the energy calculations. The reduced exposure of the phenyl groups to solvent in the tt conformation of the meso dyad compared to other accessible conformations necessitates revision of the energy calculations to take account of solvent interactions. Apart from alteration of the energy of the meso;tt conformation, the topography of the conformation energy surface is little affected by such revision. A simple, two-state rotational scheme is applicable with states at  $\varphi_t = 10^\circ$  and  $\varphi_g = 110^\circ$  for both meso and racemic dyads. The first-order interaction parameter  $\eta$  expressing the preference for the t over the g state is given by  $\eta = 0.8 (\pm 0.1) \exp(-E_\eta/RT)$  where  $E_\eta = -400 \pm 100 \text{ cal mol}^{-1}$ , the preexponential factor being evaluated from the computed conformational energy surface and  $E_\eta$  from stereochemical equilibria in polystyrene oligomers (Williams and Flory). Second-order parameters  $\omega$ ,  $\omega'$ , and  $\omega''$  for the interactions  $\text{CH}_2\text{-CH}_2$ ,  $\text{CH}_2\text{-C}_6\text{H}_5$  and  $\text{C}_6\text{H}_5\text{-C}_6\text{H}_5$ , respectively, are evaluated from the present calculations supplemented by adjustments of the energy  $E_{\omega'}$  to reproduce the observed characteristic ratio  $C_\infty$  for isotactic polystyrene. Calculated values of  $C_\infty$  and  $d \ln C_\infty/dT$  for atactic polystyrene are consistent with experimental results.

The polystyrene chain  $\text{H-}[\text{CH}_2\text{-CH}(\text{C}_6\text{H}_5)]_x\text{CH}_3$  possesses distinctive features that set it apart from polypropylene treated in the preceding paper.<sup>1</sup> The phenyl substituent has a plane of symmetry, whereas the methyl group is quasi-cylindrical. Although it is much larger than methyl in volume, its smaller dimension is less than the diameter of the methyl group. Its steric requirements differ markedly from those of the skeletal  $\text{CH}_2$  group which, as noted in the preceding paper,<sup>1</sup> resemble those of the  $\text{CH}_3$  group.

As will become apparent from examination of models (see Figure 1), these characteristics of the phenyl group have important consequences as follows.

(i) Owing to the comparatively small thickness of the phenyl group, the severe steric interactions between substituents normally occurring in the tt conformation of a meso dyad of a vinyl chain<sup>2</sup> can be diminished considerably by small displacements of the rotations  $\varphi_i$  and  $\varphi_{i+1}$  from their values (zero) for perfect staggering.

(ii) The proximity of the phenyl groups in this conformation (or in its analog, tg, for the racemic dyad) limits access of solvent molecules to the polymer chain, and, in particular, to the comparatively large phenyl groups. The energy of interaction between solvent and polymer is, therefore, appreciably dependent on conformation. The effects of this dependence must be taken into account in reckoning the conformational energy.

(iii) The  $\bar{g}$  conformation is subject to steric interactions of such severity as to obviate its consideration. (For the definition of g and  $\bar{g}$  states, see ref 3 and the preceding paper.) These steric interactions, which are identified and examined in this paper, are analogous to those found likewise to exclude the  $\bar{g}$  conformation in poly(methyl methacrylate),<sup>4</sup> wherein one of the substituents, the ester group, is planar and, hence, resembles phenyl in its spatial requirements.

In order to clarify the various interactions in polystyrene chains, we have carried out conformational energy calculations using conventional empirical methods cited in the preceding paper. The solvent interaction energy is taken into account in crude approximation. In recognition of limitations of the energy calculations, we rely on them principally to define the accessible regions of conformational space and the shapes of these domains. The estimated energies are adjusted within reasonable ranges as required to achieve agreement with experimental results on stereochemical equilibria in polystyrene oligomers and on the dimensions of isotactic and atactic polystyrene chains.

### Conformational Energies

**Geometric Data and Methods of Calculation.** Bond lengths and bond angles are given in Table I. The bond an-

Table I  
Geometrical Parameters<sup>5</sup>

| Bond   | Bond length, Å | Bond angle  | Angle, deg |
|--|----------------|---|------------|
| C–C  | 1.53           | $\angle \text{CC}^\alpha \text{C}$                                      | 112        |
|  |                | $\angle \text{C}^\alpha \text{CC}^\alpha$                               | 114        |
| $\text{C}^\alpha\text{--C}^{\text{ar}}$      | 1.51           | $\angle \text{CC}^\alpha \text{C}^{\text{ar}}$                          | 112        |
| C–H  | 1.10           | $\angle \text{CC}^\alpha \text{H}$                                      | 107        |
|  |                | $\angle \text{C}^\alpha \text{CH} = \angle \text{HCH}$                  | 110        |
|  |                | $\angle \text{C}^{\text{ar}} \text{C}^{\text{ar}} \text{H}$             | 120        |
| $\text{C}^{\text{ar}}\text{--C}^{\text{ar}}$ | 1.39           | $\angle \text{C}^{\text{ar}} \text{C}^{\text{ar}} \text{C}^{\text{ar}}$ | 120        |

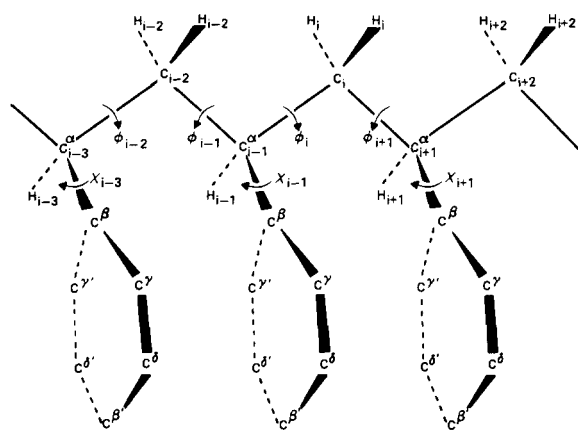


Figure 1. Portion of the isotactic polystyrene chain in the all-trans conformation.

gles were treated as fixed, the same values being assigned for all conformations.

As was shown previously,<sup>6,7</sup> the phenyl substituent is confined to orientations such that its plane is approximately perpendicular to the plane defined by the skeletal bonds flanking the carbon  $\text{C}^\alpha$  to which it is attached. Similar steric interactions affect the rotation  $\chi$  (see Figure 1) of the phenyl group in each of the preferred conformations. Repulsions between one of the ortho CH groups of phenyl and one of the H atoms of the neighboring  $\text{CH}_2$  group (e.g., between  $(\text{CH})_{i-1}^\gamma$  and  $\text{H}_i$  in Figure 1) and between the ortho CH and an atom (H) or group pendent to the adjoining  $\text{C}^\alpha$  (e.g., pendent to  $\text{C}_{i+1}$  in Figure 1) are the interactions principally responsible. The rotation is confined effectively to the range  $\chi \approx \pm 20^\circ$ , where  $\chi$  is measured from the orientation in which the phenyl group is perpendicular to the plane of the adjoining backbone bonds. A more detailed analysis of the incident interactions shows the departure of the mean value of  $\chi$  from  $0^\circ$  to be small in the preferred conformations (see below). Moreover, the range accessible to  $\chi$  is about the same in each of them. Hence, it is justified to fix  $\chi$  at  $0^\circ$ . This value was employed in all calculations reported below.

As in the preceding paper, a threefold intrinsic torsional potential having a barrier of  $2.8 \text{ kcal mol}^{-1}$  was assigned to each skeletal C–C bond. The Lennard-Jones 6–12 potential was employed for nonbonded pairs of atoms. Parameters were assigned in the manner previously described.<sup>1</sup> Parameters for the hydrogen and aliphatic carbon atom are given in Table I of the preceding paper. To the aromatic carbon atom  $\text{C}^{\text{ar}}$ , we assign a van der Waals radius  $r_i$  of  $1.95 \text{ Å}$ . This value is chosen to represent half the distance between two  $\text{C}^{\text{ar}}$  atoms at which their mutual interaction energy is minimized. It is taken to be larger than the conventional radius, ca.  $1.85 \text{ Å}$  of the aromatic carbon<sup>8</sup> derived from intermolecular distances in crystals. The larger radius is cho-

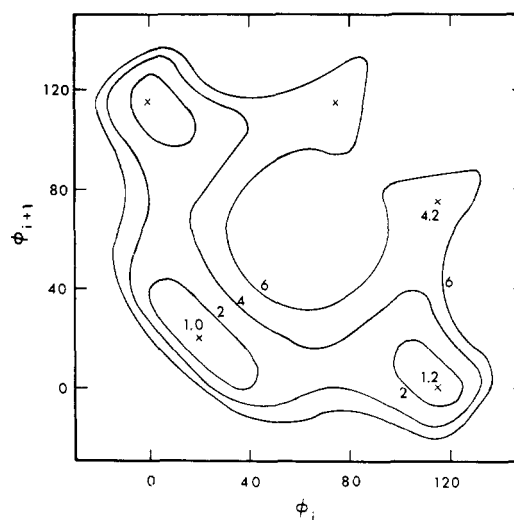


Figure 2. Conformational energy contours for a meso dyad calculated as a function of skeletal bond rotations  $\phi_i$  and  $\phi_{i+1}$ ; solvent interactions ignored; phenyl group rotations fixed at  $\chi = 0$  or  $180^\circ$ . Locations of minima are denoted by  $\times$  and the energy contours are labeled in  $\text{kcal mol}^{-1}$  relative to the energy minimum of the racemic;tt conformation. The torsional angles  $\phi_i$  and  $\phi_{i+1}$  are measured in the right- and left-handed senses, respectively.

sen in recognition of the effects of attractive interactions between other atoms of molecules in the crystalline state.<sup>2</sup> The atomic polarizability of  $\text{C}^{\text{ar}}$  is taken to be  $\alpha_i = 1.23 \text{ Å}^3$ , with an effective number  $N_i$  of electrons of five.<sup>9</sup>

In conformations in which neighboring phenyl groups are apposed, as in the tt conformation shown for the meso dyad in Figure 1, the energy of attraction between them is large. It is on the order of  $5 \text{ kcal mol}^{-1}$  according to the calculations outlined above. This energy diminishes rapidly as the distance between the atoms comprising these groups increases. In the tg conformation for the meso dyad, for example, it is quite negligible. However, the phenyl groups are then exposed to solvent molecules which provide interactions that may largely compensate the sacrifice of the phenyl–phenyl interaction.

As the distance between two proximate phenyl groups increases, we expect the energy of the system to increase at first, but to level off as the distance becomes great enough for the solvent molecules to penetrate the space between them. As a means of taking account of the compensatory effect of interactions of various parts of the chain with solvent, we let the energy between every pair of atoms  $i$  and  $j$  be represented by the 6–12 potential for distances less than some value  $\sigma$  and assume it to remain constant at the value for  $r_{ij} = \sigma$  for all distances  $r_{ij} > \sigma$ . This truncation procedure was adopted previously by Brant and Flory.<sup>10</sup> As a rough approximation, they took  $\sigma$  to be the sum of the van der Waals radii of the interacting atoms.

The value of  $\sigma$  eludes precise evaluation. Presumably, it should be no greater than the diameter of a solvent molecule, or a segment thereof. A value of 4 to  $5 \text{ Å}$  seems reasonable. Conformational energies were calculated for several values of  $\sigma$  in order to ascertain the dependence of the results on this parameter.

**Results of Energy Calculations.** Conformational energies calculated for a meso dyad without consideration of solvent–polymer interactions ( $\sigma = \infty$ ) are represented in Figure 2 as functions of the skeletal bond rotational angles  $\phi_i$  and  $\phi_{i+1}$ ; see Figure 1. Contours are shown at the energies quoted in  $\text{kcal mol}^{-1}$  relative to the minimum for the racemic;tt state (Figure 4). For the meso dyad as represented in Figure 1, bonds  $i$  and  $i + 1$  are of  $d$  and  $\ell$  chirality, re-

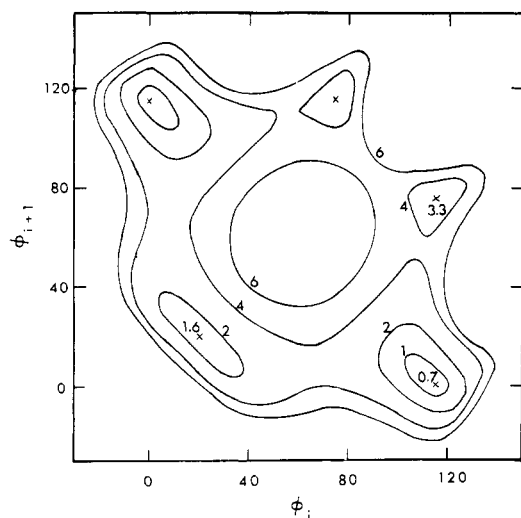


**Figure 3.** Conformational energy contours for a meso dyad computed with the 6-12 energy function truncated at  $\sigma = 5.0$  Å for all atom pairs. See legend for Figure 2.

spectively.<sup>1,3</sup> Accordingly,  $\phi_i$  is measured in the right-handed sense in Figure 2 and  $\phi_{i+1}$  in the left-handed sense.<sup>3</sup>

Energies used for construction of the contours in Figure 2 were computed at intervals of  $5^\circ$  in  $\phi_i$  and  $\phi_{i+1}$  within ranges of  $\pm 40^\circ$  of each of the minima, and at intervals of  $20^\circ$  elsewhere. Three of the five minima are readily identified as tt, tg, and gt. The gg conformation is separated into two minima with a low barrier between them. The  $\bar{g}$  conformations impose severe steric overlaps between an ortho CH group of phenyl and one of the groups bonded to the adjacent  $C^\alpha$  atom. For example, in the  $\bar{g}t$  conformation of the meso dyad in Figure 1, the  $(CH)_{i-1}^\gamma$  group impacts  $H_{i+1}$ ; similar encounters occur for a racemic dyad. Although these repulsions can be eased somewhat by rotation ( $\chi$ ) of the phenyl group, the conformational energies throughout the  $\bar{g}$  domains remain more than 5 kcal mol<sup>-1</sup> above the lowest minimum (tt). Moreover, the minima involving  $\bar{g}$  conformations are restricted to very small regions. For these reasons, the  $\bar{g}$  regions may be ignored. They are, therefore, omitted in Figure 2 and the other conformational energy diagrams to follow.

The conformations at the minima are displaced somewhat from the locations for perfect staggering. The tt minimum occurs near  $20, 20^\circ$ ; the gt and tg minima are located at  $115, 0^\circ$  and at  $0, 115^\circ$ ; and the gg state is separated into two shallow minima at  $115, 75^\circ$  and  $75, 115^\circ$  with a col of only slightly greater energy between them. The small shift in the location of the gauche state in the tg and gt conformations and the splitting of the gg conformation reflect the alleviation of second-order steric repulsions brought about by minor adjustments in  $\phi_i$  and  $\phi_{i+1}$ . These features find precedent in previous calculations on polymethylene and on other vinyl polymers.<sup>1,2,11</sup>

Recently Aylward has reported conformational energy calculations for the meso dyad of poly(*p*-styrenesulfonic acid).<sup>12</sup> Only the Coulombic interactions of the sulfonic acid groups were considered; their van der Waals interactions were not included. Although parameters used by Aylward to represent nonbonded interactions differ somewhat from those we have used, his results<sup>12</sup> resemble closely those shown in Figure 2.

The most striking result of these calculations is the appearance of the tt minimum at an energy slightly lower than that of gt or tg. Steric repulsions (second-order) be-

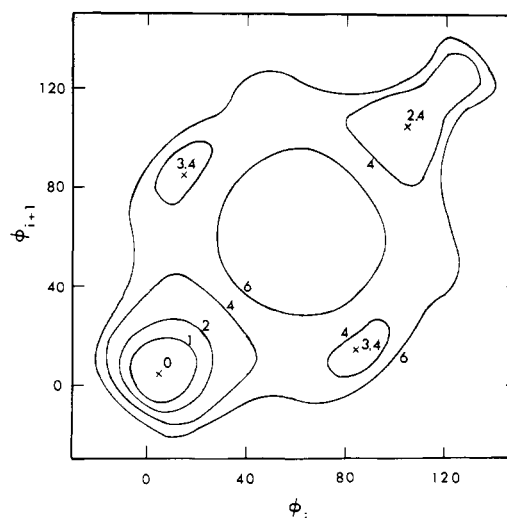


**Figure 4.** Conformational energy contours for a racemic dyad; solvent interactions neglected. For the racemic *dd* dyad,  $\phi_i$  and  $\phi_{i+1}$  are measured in the right-handed sense, and for *ll* enantiomorph in the left-handed sense.

tween substituents generally raise the energy of the former conformation well above the latter in an isotactic, or all meso, vinyl chain. It will be noted from Figure 2 that the energy for the staggered tt conformation at  $0, 0^\circ$  exceeds 6 kcal mol<sup>-1</sup>. The energy falls rapidly as the steric repulsions between the phenyl groups are relieved by small increases in  $\phi_i$  and  $\phi_{i+1}$ . This feature of the energy surface is a consequence of the planar geometry of the large phenyl group. Thus, for  $\phi_i, \phi_{i+1} = 0, 0^\circ$ , the distances  $C_{i-1}^\beta - C_{i+1}^\beta$ ,  $C_{i-1}^\gamma - C_{i+1}^\gamma$ ,  $C_{i-1}^\delta - C_{i+1}^\delta$ ,  $C_{i-1}^{\beta'} - C_{i+1}^{\beta'}$ ,  $C_{i-1}^{\gamma'} - C_{i+1}^{\gamma'}$ ,  $C_{i-1}^{\delta'} - C_{i+1}^{\delta'}$ ,  $C_{i-1}^{\gamma} - C_{i+1}^{\delta'}$ ,  $C_{i-1}^{\delta} - C_{i+1}^{\gamma'}$  are 2.60, 2.65, 2.68, 2.67, 2.62, and 2.59 Å, respectively, all much smaller than the sum, 3.9 Å, of the van der Waals radii of the interacting aromatic carbon atoms. At  $\phi_i = \phi_{i+1} = 20^\circ$ , these distances are increased to 3.07, 3.09, 3.56, 4.01, 4.00, and 3.53 Å, respectively. Repulsions between the phenyl groups are, therefore, relieved by this adjustment of the conformation. Attractions between them are large at these distances. It is for this reason that the energy at the tt minimum is lower than that for the tg or gt minima.

In the tg and gt conformations of the meso dyad, the phenyl groups are well removed from one another. Hence, their mutual interaction energy is negligible. The fact that the phenyl groups are exposed to greater numbers of solvent molecules in the tg and gt conformations is not taken into account in the calculations shown in Figure 2.

The energy surface represented in Figure 3 has been calculated using the truncated Lennard-Jones potential with  $\sigma = 5.0$  Å for all pairs of atoms. The energies are expressed relative to that for the racemic;tt minimum calculated in the same manner (see Figure 5). Comparison of Figures 3 and 2 serves to illustrate, qualitatively at least, the effects of differences in solvent interactions in the various conformations. The general characteristics of the conformational energy surfaces are similar; the locations of the minima and the sizes and shapes of the surrounding domains are virtually the same in Figure 3 as compared with Figure 2. However, the energy at the tt minimum in Figure 3 is about 0.9 kcal mol<sup>-1</sup> higher than the tg minimum. Thus, truncation of the interaction energies for atom pairs at the values for  $r_{ij} = \sigma = 5$  Å for all distances  $r_{ij} > \sigma$  increases the energy of the tt state (meso) relative to tg by 1.1 kcal mol<sup>-1</sup>. Calculations carried out with  $\sigma = 3.9$  and 7.0 Å yielded 2.4 and -0.2 kcal mol<sup>-1</sup>, respectively, for the energy of the tt mini-

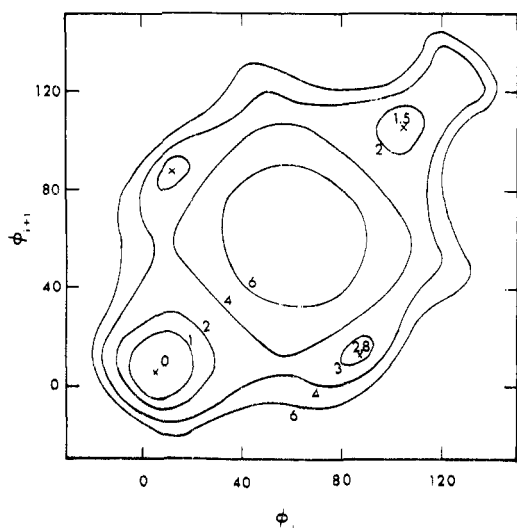


Figure 5. Conformational energy contours for a racemic dyad computed with the 6-12 energy function truncated at  $\sigma = 5.0$  Å for all atom pairs.

imum relative to the tg minimum.

Figure 4 shows the conformational energy surface for the racemic dyad calculated with use of the Lennard-Jones function for all distances  $r_{ij}$  (i.e., for  $\sigma = \infty$ ). The surface obtained with  $\sigma = 5.0$  Å is presented in Figure 5. Energies were calculated at intervals of  $5^\circ$  in  $\phi_i$  and  $\phi_{i+1}$ , in the regions of minima, and at intervals of  $20^\circ$  elsewhere, exactly as for the meso dyad. The tt minimum occurs at  $5,5^\circ$ , the gg minimum at  $105,105^\circ$ , and the gt and tg minima at  $85,10^\circ$  and  $10,85^\circ$ . The locations of these minima and the shapes of their domains are again little affected by the allowance for solvent-polymer interactions. As in the case of meso dyad, the principal effect occurs in the relative energies of the minima. The difference between the gg and tt minima is decreased from  $2.4 \text{ kcal mol}^{-1}$  in Figure 4 to  $1.5 \text{ kcal mol}^{-1}$  in Figure 5. Also to be noted is the fact that the energy for the tg and gt minima of the meso dyad relative to that for the tt minimum of the racemic dyad decreases from  $1.2 \text{ kcal mol}^{-1}$  (Figure 2) to  $0.7 \text{ kcal mol}^{-1}$  (Figure 3) as a consequence of truncation of the nonbonded interactions at their values for  $r_{ij} = \sigma = 5.0$  Å. Similar calculations carried out for  $\sigma = 3.9$  and  $7.0$  Å are not presented in detail here.

The mean values of  $\langle \phi_i \rangle, \langle \phi_{i+1} \rangle$  for each of the major dyad conformations were determined by taking averages over the respective domains according to the procedure used in the investigation of polypropylene.<sup>1</sup> The pair of minima occurring at  $115,75^\circ$  and  $75,115^\circ$  for the meso dyad, i.e., in the vicinity of its gg conformation, was treated as a single state. Inasmuch as these minima occur at an energy approximately  $3 \text{ kcal mol}^{-1}$  above the tg minima, they are of low incidence, and their representation by a single state is inconsequential. The validity of this procedure has been demonstrated for polymethylene.<sup>11,13</sup> Averaging was performed by summing over angles at intervals of  $5^\circ$ , each combination of torsional angles being weighted by the Boltzmann factor of its energy. The results of these computations carried out for several values of  $\sigma$  at  $T = 300 \text{ K}$  are presented in Table II. As expected from the similarities of the energy surfaces, the mean conformations are quite insensitive to the value of  $\sigma$ .

#### Statistical Weight Matrices

Owing to the exclusion of the g domains by the large steric repulsions occurring therein, the accessible conforma-

Table II  
Averaged Conformations  $\langle \phi_i \rangle, \langle \phi_{i+1} \rangle$  at  $T = 300 \text{ K}$

|            | $\langle \phi_i \rangle, \langle \phi_{i+1} \rangle$ , deg |                          |                   |
|------------|--|--------------------------|-------------------|
|            | $\sigma = 3.9 \text{ Å}$                                   | $\sigma = 5.0 \text{ Å}$ | $\sigma = \infty$ |
| Meso;tt    | 25,26  | 22,22                    | 22,22             |
| Meso;tg    | 7,109  | 6,110                    | 6,109             |
| Meso;gg    | 92,92  | 92,92                    | 92,92             |
| Racemic;tt | 10,10  | 9,9                      | 7,7               |
| Racemic;gg | 105,105  | 105,105                  | 105,105           |
| Racemic;tg | 22,88  | 20,87                    | 19,86             |

tional domains are small in number, and their matrix representation is correspondingly simplified. The principal conformations whose averaged locations are recorded in Table II can be represented by two statistical weight matrices of  $2 \times 2$  order, one of them for the meso and the other for the racemic dyad. They are of the form

$$U'' = \begin{bmatrix} z_{tt}'' & z_{tg}'' \\ z_{gt}'' & z_{gg}'' \end{bmatrix} \quad (1)$$

The elements are the partition functions  $z_i''$  for each of the conformational domains; see the preceding paper.<sup>1</sup> Here,  $i$  is the generic index for one of the conformations of the two dyads, e.g., for meso;tt, etc. From the point of view of rotational isomeric state (RIS) theory, eq 1 may be regarded as the matrix representation of dyad conformations in terms of combinations of states, t and g, of the individual bonds. According to the results in Table II, however, the precise location of each of these bond states depends to some extent on the state of the other member of the dyad pair, and on the stereochemical character of the dyad. Representation of the conformations according to eq 1 with states variably located as specified in Table II departs, therefore, from one of the premises of RIS theory.<sup>2</sup>

Before pursuing this minor inconsistency, we should direct attention to the significance of the  $U''$  matrix when evaluated from the dyad energy calculations above. As was observed for polypropylene,<sup>1</sup> computations thus carried out comprehend interactions of first order for both bonds and those of second order for the dyad pair. Hence, the complementary matrix  $U'$  for the pair of bonds flanking the substituted carbon,  $C^\alpha$ , must be limited to interactions of second order. Only conformations of g|g character (g being excluded for polystyrene) for this bond pair are subject to appreciable second-order interactions. Throughout the g|g domain they are intolerably severe. This is a consequence of the fact that, in addition to the repulsions between the adjoining pair of  $CH^\alpha$  members of the chain separated by four skeletal bonds, groups attached to these  $C^\alpha$  atoms ( $C_6H_5$  or  $CH_2$ ) are also subjected to steric overlaps with one, at least, of the  $CH^\alpha$  members when the skeletal conformation is g|g. This will be apparent from examination of models. It follows that a statistical weight of zero is appropriate for g|g, and that weights of unity apply to each of the other three conformations. These values being unaltered by the variations in the locations of t and g states from one dyad conformation to another, the statistical weight matrix for this bond pair may be expressed unambiguously by

$$U' = \begin{bmatrix} 1 & 1 \\ 1 & 0 \end{bmatrix} \quad (2)$$

Thus, contrary to the usual requirements of RIS theory, the locations of the bond rotational states, *t* and *g*, need not be specified uniquely in this instance.

Configurational characteristics of polystyrene can be treated in this fashion, with avoidance of approximations associated with assignment of rotational states to specific locations which are the same for all combinations. However, the advantages gained by assigning definite locations to *trans* and *gauche* states according to conventional RIS procedures outweigh the resulting errors, which in this instance are very small (see Appendix). In particular, resolution of the conformational energies into those attributable to first- and second-order interactions requires specification of *t* and *g* states, the same in all conformations in which they are involved. Rational adjustment of conformational energies for the purpose of achieving agreement with various experimental results on polystyrene and its oligomers is facilitated by allocation of the energies in this manner. The uncertainties arising from differences in solvent interactions in various conformations can be resolved more straightforwardly when interpreted in terms of the statistical weights for specific first- and second-order interactions. Hence, we employ this procedure.

The averaged conformations listed in Table II may be approximated by taking rotational states at  $\varphi_t = 10^\circ$  and  $\varphi_g = 110^\circ$ . Substantial differences compared with the calculated values of  $\langle \varphi_i \rangle, \langle \varphi_{i+1} \rangle$  occur only for *meso*;tt, *meso*;gg, and *racemic*;tg. The latter two are of high energy; hence, the discrepancies are inconsequential. The displacements of  $12^\circ$  from the averaged torsional angles for the *meso*;tt conformation become significant only to the extent that this conformation is competitive with *meso*;tg and *meso*;gt. The error involved is found to be small for acceptable values of the energy parameters (see Appendix).

In accordance with previous definitions,<sup>2,3</sup> we let  $\eta$  denote the first-order parameter expressing the statistical weight of the *trans* relative to the *gauche* state; second-order interactions between  $\text{CH}_2\text{-CH}_2$ ,  $\text{CH}_2\text{-C}_6\text{H}_5$ , and  $\text{C}_6\text{H}_5\text{-C}_6\text{H}_5$  are characterized by  $\omega$ ,  $\omega'$ , and  $\omega''$ , respectively. The statistical weight matrices for the pair of bonds within *meso* and *racemic* dyads may then be expressed as follows:

$$U_m'' = \begin{bmatrix} \omega'' & 1/\eta \\ 1/\eta & \omega/\eta^2 \end{bmatrix} \quad (3)$$

and

$$U_r'' = \begin{bmatrix} 1 & \omega'/\eta \\ \omega'/\eta & 1/\eta^2 \end{bmatrix} \quad (4)$$

after division of all elements by  $\eta^2$  in order to normalize them relative to the *racemic*;tt conformation.

Partition functions  $z_\zeta$  for each state  $\zeta$  were evaluated by numerical integration of the Boltzmann factors evaluated at intervals of  $5^\circ$  over the respective domains; see eq 4 of the preceding paper.<sup>1</sup> Calculations were carried out for a temperature of 300 K using the energy surfaces computed for  $\sigma = 3.9, 5.0 \text{ \AA}$  and  $\infty$ . These statistical weights relative to the value for *racemic*;tt are given in the second column of Table III. The average energies  $\langle E_\zeta \rangle$  calculated according to eq 5 of ref 1 are presented in the third column. The preexponential factors  $\alpha_\zeta$  defined by

$$z_\zeta = \alpha_\zeta \exp(-\langle E_\zeta \rangle/RT) \quad (5)$$

are given in the last column of Table III. All quantities are expressed relative to the *racemic*;tt state.

The relative values of  $z_\zeta$  and of  $\langle E_\zeta \rangle$  depend markedly

Table III  
Partition Functions, Average Energies,  
and Preexponential Factors for the  
Respective Conformations<sup>a,b</sup>

| State                      | $z_\zeta$ | $\langle E_\zeta \rangle$ ,<br>kcal mol <sup>-1</sup> | $\alpha_\zeta$ |
|----------------------------|-----------|---|----------------|
| $\sigma = 3.9 \text{ \AA}$ |           |   |                |
| Meso;tt                    | 0.034     | 2.61  | 2.75           |
| Meso;tg                    | 0.67      | 0.30  | 1.12           |
| Meso;gg                    | 0.020     | 2.66  | 1.71           |
| Racemic;tt                 | 1.00      | 0.00  | 1.00           |
| Racemic;tg                 | 0.021     | 2.67  | 1.83           |
| Racemic;gg                 | 0.26      | 0.98  | 1.34           |
| $\sigma = 5.0 \text{ \AA}$ |           |   |                |
| Meso;tt                    | 0.12      | 1.61  | 1.79           |
| Meso;tg                    | 0.35      | 0.73  | 1.18           |
| Meso;gg                    | 0.007     | 3.36  | 1.84           |
| Racemic;tt                 | 1.00      | 0.00  | 1.00           |
| Racemic;tg                 | 0.013     | 2.95  | 1.83           |
| Racemic;gg                 | 0.087     | 1.67  | 1.47           |
| $\sigma = \infty$          |           |   |                |
| Meso;tt                    | 0.36      | 0.91  | 1.65           |
| Meso;tg                    | 0.18      | 1.17  | 1.31           |
| Meso;gg                    | 0.002     | 4.17  | 2.02           |
| Racemic;tt                 | 1.00      | 0.00  | 1.00           |
| Racemic;tg                 | 0.006     | 3.50  | 1.93           |
| Racemic;gg                 | 0.025     | 2.48  | 1.63           |

<sup>a</sup> All values are relative to the *racemic*;tt state. <sup>b</sup> Calculations carried out for a temperature of 300 K.

on the value assigned to  $\sigma$ , according to the results in Table III. The preexponential factors  $\alpha_\zeta$ , which are measures of the effective sizes of the domains, are less affected by  $\sigma$ . This obviously is a reflection of the fact that the form of the energy surface surrounding the given minimum is, like the location of the minimum itself, insensitive to  $\sigma$ .

As in the preceding paper,<sup>1</sup> we let

$$\xi = \xi_0 \exp(-E_\zeta/RT) \quad (6)$$

where  $\xi$  is any one of the four statistical weights  $\eta$ ,  $\omega$ ,  $\omega'$ , and  $\omega''$ . The quantities  $z_\zeta$ ,  $\langle E_\zeta \rangle$ , and  $\alpha_\zeta$  in eq 5 and Table III for each conformation  $\zeta$  may be related to the appropriate combinations of the  $\xi$ ,  $\xi_0$ , and  $E_\zeta$  in eq 6 that are specified by the elements of the matrices in eq 3 and 4. We thus have at our disposal five relations between each set of four unknowns. To avoid overdetermination, we ignore the *racemic*;gg state whose statistical weight is  $\eta^{-2}$ . Use of this state instead of *meso*;tg having the statistical weight  $\eta^{-1}$  yields values of  $\eta_0$  and  $E_\eta$  differing little from those obtained in the foregoing manner and given in Table IV. The parameters  $\xi_0$  and  $E_\zeta$  obtained in this way are presented in Table IV.

The energies  $E_\eta$  and  $E_{\omega''}$  exhibit strong dependences on  $\sigma$ . On the other hand,  $E_\omega \approx 2.0 \text{ kcal mol}^{-1}$  and  $E_{\omega'} \approx 2.2 \text{ kcal mol}^{-1}$  for all values of  $\sigma$ . These observations find immediate explanation in the fact that those conformations in which consecutive phenyl groups are in close contact, namely, *meso*;tt and *racemic*;tt, bear the statistical weights  $\eta^2\omega''$  and  $\eta^2$ , respectively, before normalization. It is noteworthy that the energy  $E_\omega \approx 2.0 \text{ kcal mol}^{-1}$  associated with the second-order interactions between  $\text{CH}_2$  groups (see above) duplicates the value of  $E_\omega$  for the  $g^\pm g^\mp$  conformations in polymethylene.<sup>11</sup>

The preexponential factors are nearly independent of  $\sigma$ ,

**Table IV**  
Energies and Preexponential Factors Associated with the Statistical Weights

| $\sigma, \text{\AA}$ | Energies, kcal mol <sup>-1</sup> |            |               |                |
|----------------------|----------------------------------|------------|---------------|----------------|
|                      | $E_\eta$                         | $E_\omega$ | $E_{\omega'}$ | $E_{\omega''}$ |
| 3.9                  | -0.30                            | 2.06       | 2.37          | 2.61           |
| 5.0                  | -0.73                            | 1.90       | 2.22          | 1.61           |
| $\infty$             | -1.17                            | 1.83       | 2.33          | 0.91           |

|          | Preexponential factors |            |             |              |
|----------|------------------------|------------|-------------|--------------|
|          | $\eta_0$               | $\omega_0$ | $\omega'_0$ | $\omega''_0$ |
| 3.9      | 0.88                   | 1.32       | 1.61        | 2.75         |
| 5.0      | 0.84                   | 1.30       | 1.53        | 1.79         |
| $\infty$ | 0.77                   | 1.20       | 1.48        | 1.65         |

as expected; rounded values are  $\eta_0 = 0.8$ ,  $\omega_0 = 1.3$ ,  $\omega'_0 = 1.5$ ,  $\omega''_0 = 1.8$ . Hence, among the eight parameters,  $\eta_0$ ,  $E_\eta$ , etc., which determine the elements of the matrices  $U_m''$  and  $U_r''$  (see eq 3 and 4) at any temperature, all except  $E_\eta$  and  $E_{\omega''}$  may be evaluated in good approximation from conventional conformational energy calculations, without regard for effects of interactions with solvent. The calculations carried out for various values of  $\sigma$  serve to set limits on the plausible ranges for these two parameters as follows:  $0.9 < E_{\omega''} < 2.6$ ,  $-1.2 < E_\eta < -0.2$ , in kcal mol<sup>-1</sup>. The small difference between  $\omega$  and  $\omega'$  ( $\omega = 0.046$ ,  $\omega' = 0.038$  at 300 K) thus evaluated may be ignored. Hence, the statistical weights may be represented in good approximation by

$$\omega \approx \omega' \approx 1.3 \exp(-1000/T) \quad (7)$$

$$\omega'' \approx 1.8 \exp(-E_{\omega''}/RT) \quad (8)$$

$$\eta \approx 0.8 \exp(-E_\eta/RT) \quad (9)$$

These equations were employed in the following calculations,  $E_{\omega''}$  and  $E_\eta$  being adjusted as required to achieve agreement with experiment.

### Characteristic Ratios

Characteristic ratios  $C_n = \langle r^2 \rangle_0 / n\ell^2$  were calculated according to the matrix generation method which takes the following form when applied to the vinyl chain having a repeat unit of two bonds:<sup>2,3</sup>

$$\langle r^2 \rangle_0 = Z^{-1} S_0 \left( \prod_{k=1}^{x-1} S_k' S_k'' \right) S_x \quad (10)$$

where  $Z$  is the configuration partition function given by

$$Z = U_0 \left( \prod_{k=1}^{x-1} U_k' U_k'' \right) U_x \quad (11)$$

and the generator matrices  $G_k'$  and  $G_k''$  are defined according to

$$S_k' = (U_k' \otimes E_5) || G_k' || \quad (12)$$

Here  $E_5$  is the identity of order five and  $G$  is the generator matrix for bond  $i$  defined by<sup>2,3</sup>

$$G_i = \begin{bmatrix} 1 & 21^T T & \ell^2 \\ 0 & T & 1 \\ 0 & 0 & 1 \end{bmatrix}_i \quad (13)$$

$\ell_i$  and  $\ell_i^T$  being the column and row forms of the bond vec-

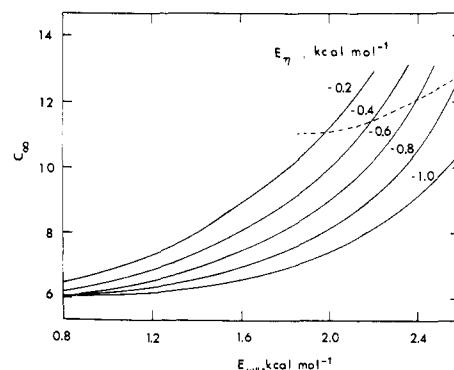


**Figure 6.** Dependence of  $C_\infty$  on  $E_\eta$  and  $E_{\omega''}$  for isotactic polystyrene at  $T = 300$  K;  $\phi_t = 10^\circ$  and  $\phi_g = 110^\circ$ .

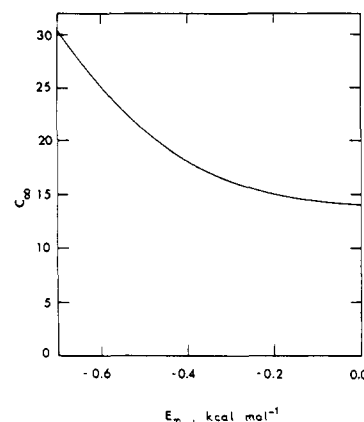


**Figure 7.** Dependence of  $C_\infty$  on  $E_\eta$  for syndiotactic polystyrene at  $T = 300$  K;  $\phi_t = 10^\circ$  and  $\phi_g = 110^\circ$ .

tor;  $T_i$  is the transformation relating the Cartesian coordinate system for bond  $i + 1$  to that for bond  $i$ .<sup>2</sup> In eq 12,  $||G_k'||$  is the diagonal array of the generator matrices  $G_k'$  for each of the two rotational states,  $t$  and  $g$ , of the first bond of the  $k$ th dyad. The matrix  $G_k''$  is equivalently defined for the second bond of the  $k$ th dyad. The terminal  $U$  and  $G$  matrices are defined by

$$\begin{aligned} U_0 &= \text{row}(1, 0) \\ U_x &= \text{col}(1, 1) \end{aligned} \quad (14)$$

and

$$\begin{aligned} G_0 &= U_0 \otimes G_1 \\ G_x &= U_x \otimes G_x \end{aligned} \quad (15)$$

where  $G_1$  is the first row of  $G$  for the first bond and  $G_x$  is the last column of  $G$  for the final bond of the chain of  $x$  units.

**The Isotactic Chain.** In Figure 6,  $C_\infty = \lim_{n \rightarrow \infty} C_n$  for isotactic polystyrene is plotted against  $E_{\omega''}$  for the several values of  $E_\eta$  indicated. The calculations were carried out for rotational isomeric states situated at  $\phi_t = 10^\circ$  and  $\phi_g = 110^\circ$ , the temperature being 300 K. The characteristic ratio increases with both  $E_\eta$  and  $E_{\omega''}$ . This behavior reflects the fact that the reductions in both  $\eta$  and  $\omega''$  brought about by increases in these energies favor the  $tg$  and  $gt$  conformations, perpetuation of either of which generates sequences of  $3_1$  helices. Although the preference for  $tg$ , or  $gt$ , is weak, it is sufficient for the incipience of these helical sequences to dominate the behavior of  $C_\infty$ . Inasmuch as the contribution of the  $gg$  state is negligible because of its high energy,  $C_\infty$  depends essentially on the sum  $E_\eta + E_{\omega''}$ . That this should be so will be apparent from eq 3. According to ex-

Table V  
Characteristic Ratios and Temperature  
Coefficients for Atactic Polystyrene  
with  $w_m = 0.50$  at  $T = 300$  K

| Energies,<br>kcal mol <sup>-1</sup> |          | $C_\infty$ | $(d \ln C_\infty/dT) \times 10^3$ |
|-------------------------------------|----------|------------|-----------------------------------|
| $E_{\omega''}$                      | $E_\eta$ |            |                                   |
| 2.0                                 | -0.2     | 7.75       | -0.47                             |
| 2.2                                 | -0.4     | 8.63       | -0.73                             |
| 2.4                                 | -0.6     | 9.50       | -0.90                             |
| 2.6                                 | -0.8     | 10.23      | -0.90                             |

periments,  $C_\infty \approx 11$  for isotactic polystyrene.<sup>14,15</sup> Hence, we infer that  $E_{\omega''} + E_\eta \approx 1.8$  kcal mol<sup>-1</sup>. The dashed line in Figure 6 represents  $C_\infty$  as a function of  $E_\eta$  when  $E_{\omega''} + E_\eta$  is fixed at this value.

The greater incidence of the tt state according to the present treatment admits of lower values of  $C_\infty$  for isotactic polystyrene than were predicted previously.<sup>2</sup>

**The Syndiotactic Chain.** The characteristic ratio for syndiotactic polystyrene calculated for  $T = 300$  K is shown in Figure 7 as a function of  $E_\eta$ . The statistical weights were evaluated according to eq 7 and 9. Rotational states were taken at  $\varphi_t = 10^\circ$  and  $\varphi_g = 110^\circ$  as above. The characteristic ratio increases as  $E_\eta$  decreases and, therefore, as the occurrence of the tt conformation is enhanced.

Experimental results for comparison with these calculations are not available.

**The Atactic Chain.** Two sets of Monte Carlo chains consisting of 200 units were generated with Bernoullian distributions of meso and racemic dyads. In one the expectation  $w_m$  of meso dyads was 0.50; in the other it was 0.30. Each set consisted of 20 chains. Conventional atactic polystyrenes are believed to fall within this range.<sup>16,17</sup> Characteristic ratios were calculated using the parameters specified above with  $E_\eta + E_{\omega''}$  set equal to 1.8 kcal mol<sup>-1</sup>, as required to reproduce  $C_\infty$  for isotactic polystyrene. Results for  $w_m = 0.50$  at a temperature of 300 K are presented in Table V. Those for chains with  $w_m = 0.30$  are given in Table VI. The experimental value,<sup>15,18-20</sup>  $C_\infty \approx 10.0$ , suggests  $E_\eta = -0.4 \pm 0.4$  kcal mol<sup>-1</sup> and  $E_{\omega''} = 2.2 \mp 0.4$  kcal mol<sup>-1</sup>.

Temperature coefficients of  $\langle r^2 \rangle_0$  evaluated for atactic polystyrene from calculations at 350 K in conjunction with those at 300 K are given in the last columns of Tables V and VI. They are consistently negative, but variable in magnitude, depending on  $w_m$  and the choice of  $E_\eta$  and  $E_{\omega''}$ . Further calculations not presented here fail to produce a positive temperature coefficient for any admissible combination of these energies.

Thermoelastic measurements on cross-linked polystyrene networks and viscometric measurements on dilute polystyrene solutions carried out by Ciferri and Orofino et al.<sup>21-24</sup> indicated a small, positive coefficient,  $d \ln C_\infty/dT \approx 0.4 \times 10^{-3}$  deg<sup>-1</sup>. Recently, Kuwahara and coworkers<sup>25</sup> have reported intrinsic viscosities of atactic polystyrene in cyclopentane at the  $\theta$  points, 154.2 and 19.6°C, associated with lower and upper critical phase separation. Their results yield  $d \ln C_\infty/dT = -0.1 \times 10^{-3}$  deg<sup>-1</sup>. Neutron scattering results of Benoit and coworkers<sup>26</sup> on dilute mixtures of protonated polystyrene with the deuterated polymer at 36°C and at 120°C suggest that  $d \ln C_\infty/dT$  is negative. Our calculations are consistent with these negative values. They cannot be reconciled with the earlier positive coefficients.

**Stereochemical Equilibria in Oligomers of Polysty-**

Table VI  
Characteristic Ratios and Temperature  
Coefficients for Atactic Polystyrene  
with  $w_m = 0.30$  at  $T = 300$  K

| Energies,<br>kcal mol |          | $C_\infty$ | $(d \ln C_\infty/dT) \times 10^3$ |
|-----------------------|----------|------------|-----------------------------------|
| $E_{\omega''}$        | $E_\eta$ |            |                                   |
| 2.0                   | -0.2     | 9.00       | -0.28                             |
| 2.2                   | -0.4     | 10.46      | -0.83                             |
| 2.4                   | -0.6     | 12.23      | -1.32                             |
| 2.6                   | -0.8     | 14.02      | -1.52                             |

rene. The equilibria between the diastereoisomers of 2,4-diphenylpentane (DPP) and between those of 2,4,6-triphenylheptane (TPH) were investigated by Williams and Flory.<sup>27</sup> The equilibria depend almost exclusively on  $\eta$ , the second-order parameters  $\omega$ ,  $\omega'$ , and  $\omega''$  being of little importance. The results yield values of  $\eta$  of unparalleled accuracy. From their measurements on DPP and TPH, Williams and Flory<sup>27</sup> found  $\eta = 1.5 \pm 0.1$  at 25°C and  $1.4 \pm 0.1$  at 70°C. Combining these values with the preexponential factor  $\eta_0 = 0.8$  (see eq 9) as given reliably by the conformational energy calculations, we obtain  $E_\eta = -0.38 \pm 0.10$  kcal mol<sup>-1</sup>. This value falls within the range estimated from the characteristic ratio of the atactic polymer. In accuracy it surpasses the former rough estimate, however.

We conclude, therefore, that

$$\eta = 0.8 (\pm 0.1) \exp[200 (\pm 50)/T] \quad (16)$$

This relation replaces

$$\eta = 0.5 \exp(350/T) \quad (17)$$

offered by Williams and Flory.<sup>27</sup> Both relations reproduce the stereochemical equilibria at 25 and at 70°C within limits of experimental error. The parameters in eq 17 were chosen on the basis of conformer populations in the diastereomeric oligomers as estimated from NMR coupling constants determined at various temperatures.<sup>28,29</sup> The errors attending this method are believed to render eq 17 less reliable than 16.

**Acknowledgment.** This work was supported by the Directorate of Chemical Sciences, U.S. Air Force Office of Scientific Research Grant No. AFOSR-73-2441-A-B.

## Appendix

As we have pointed out in the text, the conformational characteristics of the polystyrene chain are such as to permit rigorous analysis of its configuration-dependent properties without resolving its dyad conformations into combinations of discrete states for individual bonds. Adopting procedures indicated previously,<sup>2,3</sup> we formulate a matrix  $G_k$  for the  $k$ th dyad that joins both  $G_k'$  and  $G_k''$  with  $U_k''$  according to the following specification

$$G_k = ||G_k'|(U_k'' \otimes E_5)||G_k''| \quad (18)$$

$$= \begin{bmatrix} z_{tt}''(G'G'')_{tt} & z_{tg}''(G'G'')_{tg} \\ z_{gt}''(G'G'')_{gt} & z_{gg}''(G'G'')_{gg} \end{bmatrix} \quad (19)$$

Here  $(G'G'')_\zeta$  is the product of the  $G'$  and  $G''$  matrices for the dyad conformation denoted by  $\zeta$  and assigned the torsional angles obtained by averaging over domain  $\zeta$  (see Table II). Additionally, we define

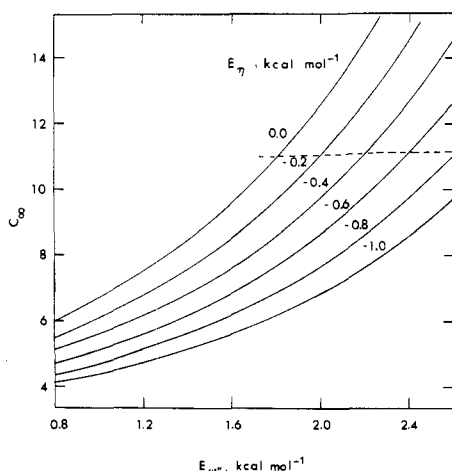


Figure 8. Dependence of  $C_\infty$  on  $E_\eta$  and  $E_{\omega''}$  for isotactic polystyrene at  $T = 300$  K according to eq 21.

$$u' = U' \otimes E_5 \quad (20)$$

Then

$$\langle r^2 \rangle_0 = Z^{-1} G_0 \left( \prod_{k=1}^{x-1} u' G_k \right) G_x \quad (21)$$

where  $G_0$  and  $G_x$  retain their previous definitions according to eq 15.

Computations were carried out for isotactic polystyrene with  $G'_\zeta$  determined by the average torsional rotation  $\langle \varphi_i \rangle$  and  $G''_\zeta$  by  $\langle \varphi_{i+1} \rangle$  using the values of these angles recorded in Table II for each conformation  $\zeta$ . Literal adherence to this procedure would dictate that conformational partition functions  $z_\zeta$  evaluated from the energy surfaces (see Table III) be used in eq 19 and for the calculation of  $Z$ . Inasmuch as the values of  $\langle \varphi_i \rangle$  and  $\langle \varphi_{i+1} \rangle$  are virtually independent of the parameters (e.g., of  $\sigma$ ) governing the energy, it is legitimate to evaluate the conformational partition functions  $z_\zeta$  from the statistical weight parameters given by eq 7–9. This procedure permits rational variation of the relative energies through manipulation of  $E_\eta$  and  $E_{\omega''}$ . Errors arising therefrom are insignificant.

Results of these computations are presented in Figure 8. A close resemblance to the curves calculated using the RIS scheme and shown in Figure 6 is apparent. Significant differences appear only for combinations of the energies such

that  $E_{\omega''} + E_\eta < 1.0$  kcal mol $^{-1}$ . For smaller values of this sum the contribution of the tt conformation is sufficiently enhanced to cause its displacement from 22,22° to 10,10° to affect the results appreciably, as close comparison of Figure 6 with Figure 8 shows. The characteristic ratio depends principally on the sum  $E_\eta + E_{\omega''}$ , as observed in Figure 6. Agreement with experiment is again achieved with  $E_\eta + E_{\omega''} \approx 1.8$  kcal mol $^{-1}$ . The locus of points meeting this condition is shown by the dashed line in Figure 8.

## References and Notes

- (1) U. W. Suter and P. J. Flory, *Macromolecules*, **8**, 765 (1975).
- (2) P. J. Flory, "Statistical Mechanics of Chain Molecules", Interscience, New York, N.Y., 1969; see also, *Macromolecules*, **7**, 381 (1974).
- (3) P. J. Flory, P. R. Sundararajan, and L. C. DeBolt, *J. Am. Chem. Soc.*, **96**, 5015 (1974); Y. Fujiwara and P. J. Flory, *Macromolecules*, **3**, 280 (1970); P. J. Flory and Y. Fujiwara, *ibid.*, **2**, 315 (1969).
- (4) P. R. Sundararajan and P. J. Flory, *J. Am. Chem. Soc.*, **96**, 5025 (1974).
- (5) H. J. M. Bowen and L. E. Sutton, "Tables of Interatomic Distances and Configurations in Molecules and Ions", The Chemical Society, London, 1958.
- (6) Y. Abe, A. E. Tonelli, and P. J. Flory, *Macromolecules*, **3**, 294 (1970).
- (7) A. E. Tonelli, *Macromolecules*, **6**, 682 (1973).
- (8) A. I. Kitaigorodskii, "Organic Chemical Crystallography", Consultants Bureau, New York, N.Y., 1961.
- (9) J. Ketelaar, "Chemical Constitution", Elsevier, New York, N.Y., 1958.
- (10) D. A. Brant and P. J. Flory, *J. Am. Chem. Soc.*, **87**, 2791 (1965).
- (11) A. Abe, R. L. Jernigan, and P. J. Flory, *J. Am. Chem. Soc.*, **88**, 631 (1966).
- (12) N. N. Aylward, *J. Polym. Sci., Polym. Chem. Ed.*, **13**, 373 (1975).
- (13) P. J. Flory, *J. Polym. Sci., Polym. Phys. Ed.*, **11**, 621 (1973).
- (14) W. R. Krigbaum, D. K. Carpenter, and S. Newman, *J. Phys. Chem.*, **62**, 1586 (1958).
- (15) M. Kurata and W. H. Stockmayer, *Fortshr. Hochpolym.-Forsch.*, **3**, 196 (1963).
- (16) F. A. Bovey, F. P. Hood, E. W. Anderson, and L. C. Snyder, *J. Chem. Phys.*, **42**, 3900 (1965).
- (17) L. F. Johnson, F. Heatley, and F. A. Bovey, *Macromolecules*, **3**, 175 (1970).
- (18) W. R. Krigbaum and P. J. Flory, *J. Polym. Sci.*, **11**, 37 (1953).
- (19) T. Altares, D. P. Wyman, and V. R. Allen, *J. Polym. Sci., Part A-2*, **4533** (1964).
- (20) T. A. Orofino and J. W. Mickey, Jr., *J. Chem. Phys.*, **38**, 2513 (1963).
- (21) T. A. Orofino and A. Ciferri, *J. Phys. Chem.*, **68**, 3136 (1964); T. A. Orofino, *J. Chem. Phys.*, **45**, 4310 (1966).
- (22) A. Ciferri, *J. Polym. Sci., Part A*, **2**, 3089 (1964).
- (23) K. Dušek, *Collect. Czech. Chem. Commun.*, **32**, 2264 (1967).
- (24) J. E. Mark, *Rubber Chem. Technol.*, **46**, 593 (1973).
- (25) N. Kuwahara, S. Saeki, S. Konno, and M. Kaneko, *Polymer*, **15**, 66 (1974).
- (26) H. Benoit, *Polym. Prepr., Am. Chem. Soc., Div. Polym. Chem.*, **15**, 324 (1974); J. P. Cotton, D. Decker, H. Benoit, B. Farnoux, J. Higgins, G. Jannik, R. Ober, C. Picot, and J. des Cloizeaux, *Macromolecules*, **7**, 863 (1974).
- (27) A. D. Williams and P. J. Flory, *J. Am. Chem. Soc.*, **91**, 311 (1969).
- (28) H. Pivovara, M. Kolinsky, D. Lim, and B. Schneider, *J. Polym. Sci., Part C*, **22**, 1093 (1969).
- (29) T. Moritani and Y. Fujiwara, *J. Chem. Phys.*, **59**, 1175 (1973).